IEEE Access
Multidisciplinary | Rapid Review | Open Access Journal

Received July 17, 2018, accepted August 14, 2018, date of publication August 30, 2018, date of current version September 21, 2018.

Digital Object Identifier 10.1109/ACCESS.2018.2867836

Ground Plane Alterations for Design of High-Isolation Compact Wideband MIMO Antenna

MUHAMMAD AZIZ UL HAQ AND SLAWOMIR KOZIEL, (Senior Member, IEEE)
Engineering Optimization and Modeling Center, School of Science and Engineering, Reykjavík University, 101 Reykjavík, Iceland

Corresponding author: Slawomir Koziel (koziel@ru.is)

This work was supported in part by the Icelandic Centre for Research (RANNIS) under Grant 174114051 and in part by the National Science Centre of Poland under Grant 2014/15/B/ST7/04683.

ABSTRACT In this paper, a simple technique for improving element isolation in wideband multiple-input multiple-output (MIMO) antenna is investigated. We consider n-section rectangular slits below the feed line and analyze the effects of the number of sections on achievable isolation. The effect of the slits is indirect by improving the impedance matching, which creates a room for isolation enhancement through rigorous optimization of all antenna parameters. The results obtained for an exemplary antenna structure indicate the advantages of increasing the slit complexity as well as a saturation effect beyond $n = 3$. Using these considerations, a compact MIMO antenna is developed and optimized to operate in the ultrawideband (UWB) (3.1–10.6 GHz) frequency range. The final design features $|S_{11}| \leq -10$ dB and isolation $|S_{21}| \leq -20$ dB in the entire UWB range, as well as small dimensions of only 25×32 mm^2. Excellent performance figures, including envelop coefficient correlation (< 0.005), diversity gain (> 9.99 dB), and total efficiency ($> 80\%$ by average), demonstrate that the considered structure is suitable for practical applications and competitive to the state-of-the-art antennas reported in the literature. Experimental validation of the design is also provided.

INDEX TERMS EM-simulation-driven design, ground plane alterations, MIMO antenna, size reduction.

I. INTRODUCTION

Wideband antennas have gained popularity owing to their attractive features such as high data rate, simultaneous multi-channel connectivity, low power consumption as well as ability to provide high-resolution images [1], [2]. The Federal Communications Commission (FCC) authorized the frequency range (3.1 – 10.6 GHz) for ultrawideband (UWB) systems to be used for commercial applications in 2002 [3], which started advancements towards development of UWB antennas for wideband applications such as wearable devices [4], Internet of Things [5], and cognitive radio [6]. However, the critical issue associated with UWB systems is their suitability for a short range communication only, which is due to low power transmission allowed by FCC. Furthermore, considerable environmental scattering causes a multipath fading that leads to degradation of the transmission quality. Finally, a single wideband antenna has its own limitations in handling multi-channel communication over a wide range.

A multiple-input-multiple-output (MIMO) technology has been used to overcome the aforementioned problems. An important characteristic of MIMO structures is separation between the antenna elements, high level of which is essential to avoid mutual coupling and to ensure reliable communication [7], [8]. Also, stronger mutual coupling between the antenna elements results in decreasing the data transfer capacity and efficiency of the MIMO system [9]. Notably, this phenomenon becomes more pronounced in compact communication systems where a limited space is allocated to mount the antenna on. Consequently, design of compact MIMO antennas with high isolation for space-limited communication devices is a considerable challenge. From the system point of view, isolation level of –20 dB is considered sufficient in the context of quality of wireless communication [9]. Yet, achieving it while maintaining the compact size of the antenna structure along with sufficient levels of other performance figures is a considerable design a challenge.

There have been significant research efforts observed over the last few years to deal with mutual coupling issues. The most popular approach is to place antenna elements orthogonal to each other [10], [11], which makes it easy to handle mutual coupling. However, orthogonally-allocated

antenna structures increase complexity of the feeding structure in compact communication devices. Other techniques to improve isolation include utilization of parasitic structures [12], Electromagnetic Band Gap (EBG) structures [13], neutralizing lines [14], and Defected Ground Structures (DGS) [15]. Although the aforementioned techniques are very attractive in the context of isolation improvement, their implementation for wideband and ultra wideband applications is difficult, especially for contemporary communication devices. Therefore, these techniques have not yet been in practical use in UWB-MIMO antenna structures to the best of authors' knowledge.

Alternative methods include a wide range of ground plane alterations. In [16], a compact UWB-MIMO antenna with F-shaped stubs in the ground plane has been proposed. High isolation ($|S_{21}| < -20$ dB) is achieved by the stub evolution in the ground plane. In [17], a bi-planar Yagi-like MIMO antenna has been proposed with isolation better than −17 dB. Two L-shape inverted parasitic strips with smaller L-shape stubs have been introduced in [18] to achieve improved isolation. The main problem associated with the above structures is their large size, as well as the fact that element isolation is not explicitly handled in the design process, therefore, it is only a byproduct of the introduced modifications. To achieve better control, explicit formulation of requirements concerning relevant performance figures is necessary along with suitable geometry alterations that are capable of controlling respective characteristics. At the same time, rigorous optimization needs to be carried out so as to account for parameter and antenna responses interrelations.

In this paper, a technique for element isolation improvement in compact UWB-MIMO antennas is proposed and investigated. Our approach involves introduction of n-section slits below the feed line. The slits permit impedance matching improvement of individual antenna elements [19], which is further utilized to enhance isolation through rigorous constrained optimization of all antenna elements and balancing reflection level (at –10 dB within the operating band of the antenna) and isolation (at –20 dB), while maintaining the compact footprint. The number $n = 2$ of the slit sections has been found to be the best compromise between efficiency (in terms of isolation improvement but also maintaining the small size) and structural complexity. The presented concept has been demonstrated for a UWB-MIMO structure based on two monopole antenna elements, placed parallel to each other with a common ground plane. Inverted L-shape stubs are utilized in the ground plane to enhance the matching. The simulated and measured results confirm the applicability of the considered antenna for contemporary modern communication devices, among others, due to its very low ECC and high diversity gain.

II. BENCHMARK MIMO ANTENNA STRUCTURE AND ANALYSIS

Our considerations are illustrated using the UWB-MIMO antenna shown in Fig. 1. Two monopole antenna elements

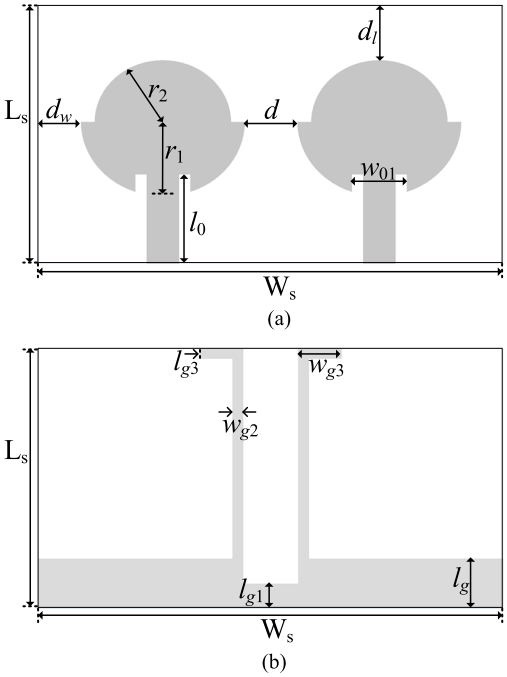

FIGURE 1. The geometry of a compact UWB-MIMO Antenna I used to demonstrate the proposed isolation enhancement concept. (a) Top and (b) Bottom view.

are positioned parallel to each other with a common ground plane and fed by 50 Ω impedance lines.

The structure is implemented on 1.55-mm-thick FR-4 substrate with $\varepsilon_r = 4.3$. The antenna geometry is described using the following vector of parameters: $\boldsymbol{x}_0 = [l_g\ l_0\ r_1\ r_2 d\ d_l\ d_w\ l_{g1}\ w_{g2}\ l_{g3}\ w_{g3}\ w_{01}]^T$. The numerical values are $\boldsymbol{x}_0^{(0)} = [3\ 5.7\ 7\ 0.9\ 7\ 3\ 3\ 0.3\ 0.2\ 0.5\ 2\ 5]^T$ mm. The computational model is implemented in CST Microwave Studio [20] (~770,000 mesh cells, simulation time 2 minutes). In order to ensure reliable experimental validation, the model includes the SMA connectors. The antennas are supposed to operate in the UWB frequency range (3.1 GHz to 10.6 GHz). Figure 2(a) shows the reflection response of the initial design which is not satisfying the condition $|S_{11}| \leq -10$ dB. Therefore, our first goal was to optimize the antenna for the maximum in-band reflection not exceeding –10 dB. Here, a pattern search algorithm [21] has been utilized with reflection constrained handled implicitly (through a penalty function approach [22]). The reflection response of optimized antenna is shown in Fig. 2(b) which indicates that

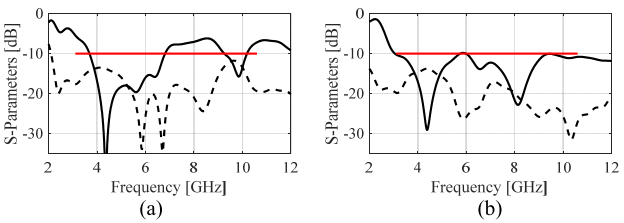

FIGURE 2. Simulated S-parameters of Antenna I: (–) S_{11}, and (– – –) S_{21}. (a) The initial design, (b) Optimized design.

the MIMO antenna is operating for entire UWB frequency range (3.1 GHz to 10.6 GHz). The numerical values of optimized antenna (called Antenna I) are as follows: $\boldsymbol{x}_1^{(0)} = [4.0\ 5.8\ 6.7\ 0.9\ 2.9\ 5.6\ 3.3\ 0.5\ 1.5\ 1.2\ 1.0\ 3.5]^{\mathrm{T}}$.

III. ANTENNA EVOLUTION TOWARDS ISOLATION IMPROVEMENT

A proposed way of improving element isolation are multi-section slits below the feel lines. To analyze the impact of these ground plane alterations on the UWB-MIMO antenna, the optimized Antenna I has undergone systematic modifications. At the first stage, a rectangular slit below the feed line was introduced as shown in Fig. 3(a) (the structure referred to as Antenna II). Upon applying this modification, the design variable vector was extended to $\boldsymbol{x}_2 = [l_g\ l_0\ r_1\ r_2d\ d_l\ d_w\ l_{g1}\ w_{g2}\ l_{g3}\ w_{g3}\ w_{01}\ l_1\ w_1]^T$. Here, l_1 and w_1 are the length and width of the introduced slit below the feed line. Antenna II was optimized using the same procedure as described before. For a fair comparison between the isolation of Antenna I and Antenna II, the overall antenna size was fixed during the optimization. The S-parameters of Antenna II are shown in Fig. 4 (a). It can be observed that isolation (S_{21}) between the two ports of the MIMO antenna elements was improved considerably. The optimized numerical values of Antenna II are: $\boldsymbol{x}_2^{(0)} = [4.6\ 5.5\ 7.0\ 0.9\ 1.2\ 5.0\ 2.9\ 0.6\ 2.0\ 1.8\ 2.2\ 3.7\ 2.6\ 1.9]^T$.

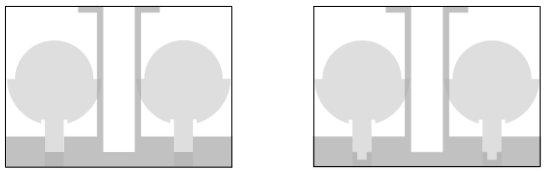

FIGURE 3. Evolution progression of the considered UWB-MIMO antenna. The ground plane is shown using the dark gray shade. (a) Antenna II, (b) Antenna III.

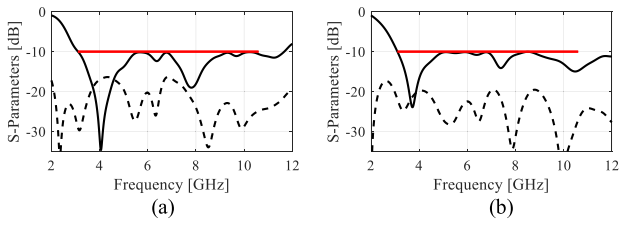

FIGURE 4. Simulated S-parameters of optimized UWB-MIMO antenna. (–) S_{11}, and (– – –) S_{21}. (a) Antenna II, (b) Antenna III.

At the next stage, another section of the slit has been added as shown in Fig. 3(b) (the structure referred to as Antenna III). The design variable vector of Antenna III is $\boldsymbol{x}_3 = [l_g\ l_0\ r_1\ r_2d\ d_l\ d_w\ l_{g1}\ w_{g2}\ l_{g3}\ w_{g3}\ w_{01}\ l_1\ w_1\ l_2\ w_2]^T$. Again, the same optimization procedure with fixed antenna size was performed. Figure 4(b) shows the S-parameters of the optimized Antenna III. The results clearly indicate that two-section slit below the feed line makes a dramatic impact on isolation ($|S_{21}| \leq -20$ dB) as compared to Antenna II. The numerical values of geometry parameters are: $\boldsymbol{x}_3^{(0)} = [5.7\ 7.0\ 7.4\ 0.8\ 1.3\ 5.4\ 0.7\ 1.0\ 3.0\ 4.2\ 1.8\ 4.2\ 3.8\ 0.2\ 0.9\ 0.8]^T$.

Further increase of the number of slit sections does not bring noticeable improvement of the isolation, therefore, Antenna III is considered a final design. Other performance figures such as total efficiency, Envelop Coefficient Correlation, and diversity gain have also been considered for all antenna structures. The purpose of this study was to analyze the impact of antenna modifications on the mentioned characteristics. Figure 5 shows the total efficiency of all antennas for the entire UWB frequency range. The average efficiency is similar for all antenna structures and larger than 80% and despite high-loss substrate (FR-4). One of the critical performance figures of a MIMO antenna, reflecting the signal correlation, is the Envelop Correlation Coefficient (ECC). For an ideal MIMO antenna, ECC value should be zero, however, ECC < 0.5 is considered acceptable for an uncorrelated MIMO antenna system. The ECC can be calculated using the field radiation pattern [23] as:

$$ECC = \frac{\left|\iint_{4\pi} [\vec{F}_1(\theta, \Phi) . \vec{F}_2(\theta, \Phi)] d\Omega\right|^2}{\iint_{4\pi} |\vec{F}_1(\theta, \Phi)|^2 d\Omega \iint_{4\pi} |\vec{F}_2(\theta, \Phi)|^2 d\Omega} \quad (1)$$

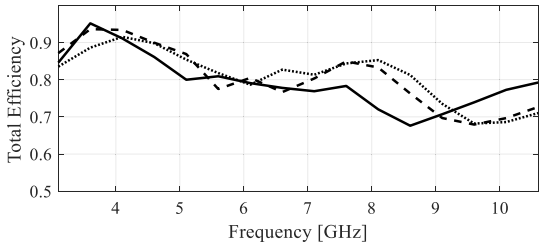

FIGURE 5. Simulated efficiencies of the optimized antennas: Antenna I (...), Antenna II (- - -), and Antenna III (–).

Where, $\vec{F}_i(\theta, \Phi)$ is the field radiation pattern of the MIMO antenna element when port i is excited (here, $i = 1, 2$) and other port is terminated with the 50Ω load. Figure 6(a) shows the ECC for Antennas I through III. Here, again, isolation-improvement-oriented antenna modification did not degrade the ECC within the entire UWB frequency range.

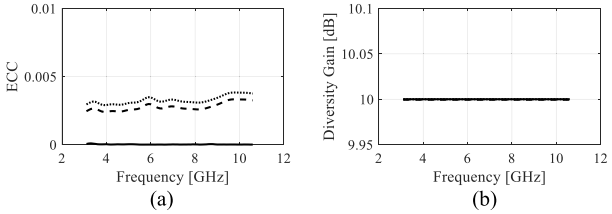

FIGURE 6. Simulated response of the optimized antennas: Antenna I (...), Antenna II (- - -), and Antenna III (–). (a) ECC, (b) Diversity Gain.

Diversity gain of the MIMO antenna can be calculated using the following equation:

$$DG = 10\sqrt{(1 - ECC^2)} \quad (2)$$

Figure 6(b) shows DG for all considered antennas. As before, improving isolation through ground plane modifications is not achieved at the expense of DG degradation.

A. CURRENT DISTRIBUTIONS

The impact of the considered ground plane alteration on antenna isolation was further analyzed using the surface current distribution over the modified MIMO antennas at 3.1 GHz as shown in Fig. 7. It is clear from Fig. 7(a) that with Port 1 excited, a significant amount of current is coupled along Port 2. This coupling effect is reduced by one-section slit below the feed line up as shown in Fig. 7(b). Introduction of the two-section slit improves the situation dramatically as illustrated in Fig. 7(c). Only a negligible amount of current is observed at the surface of the second antenna. Consequently, high isolation is achieved.

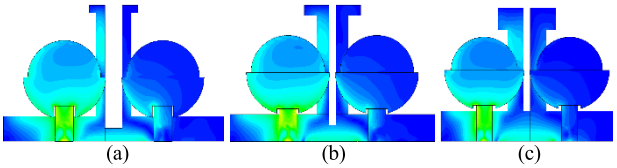

FIGURE 7. Surface current distribution at 4.1 GHz: (a) initial design, (b) design with a one-section slit, and (c) design with a two-section slit below the feed line.

B. EXPERIMENTAL VALIDATIONS

To verify the performance of the antenna, the optimized UWB-MIMO structure was fabricated (cf. Fig. 8). During the measurement process, Port 1 was excited, while Port 2 was terminated with a 50 Ω load. Figure 9 shows the measured and simulated S-parameters of the considered antenna.

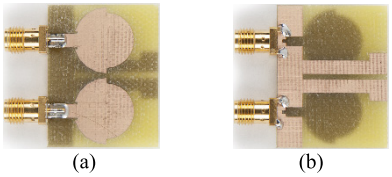

FIGURE 8. Photographs of the fabricated UWB-MIMO antenna: (a) top view, (b) bottom view.

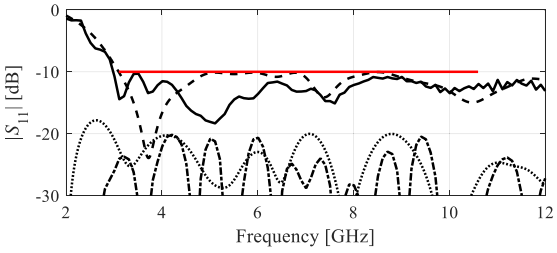

FIGURE 9. Simulated and measured S-parameters of the optimized UWB-MIMO antennas with the two-section slit below the feed line: S_{11} simulated (- - -), S_{11} measured (—), S_{21} simulated (...) and S_{21} measured (– – –).

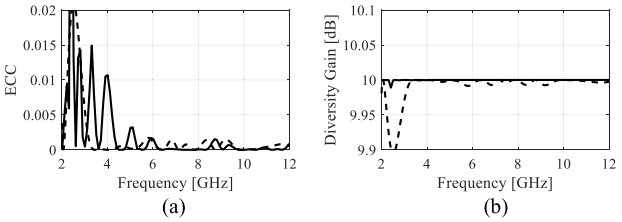

FIGURE 10. Simulated (- - -) and measured (—) response of the optimized UWB-MIMO antenna (a) Envelop Correlation Coefficient (b) Diversity Gain.

The measured results confirm the capability of the design to operate within the UWB range. A slight discrepancy might be due to fabrication tolerance and inconsistency of the the dielectric constant of the substrate. Figure 10 shows the simulated and measured ECC and DG of the antenna. As our experimental facilities do not allow to measure the 3D field pattern, the measured scattering parameters has been used for ECC evaluation using the expression [23]:

$$ECC = \frac{\left|S_{11}^{*}S_{12} + S_{21}^{*}S_{22}\right|^{2}}{\left(1 - |S_{11}|^{2} - |S_{21}|^{2}\right)\left(1 - |S_{12}|^{2} - |S_{22}|^{2}\right)} \quad (3)$$

It is clear from the Fig. 10 that ECC is lower than 0.005 and DG is higher than 9.99 dB for the entire UWB range. The important observation is that the ECC and DG responses by using the field radiation pattern or scatterinr parameters are well aligned over the entire frequency range. The considered antenna can be a good candidate for modern cammunication devices due to very low ECC and high DG. To the best of authors knowledge, the antenna exhibits a much better performance (especially, in terms of ECC and DG) than recently reported designs [16]–[18], [24]–[26] for the UWB range. The detailed performance comparison has been provided in Table 1. For a fair comparison, only parallel-fed antenna designs were considered. Figure 11 shows the simulated and measured total efficiency of the antenna. The measured results indicate that the average efficiency of the antenna is higher than 80% which also confirms the applicability of the structure for modern communication devices. Another important characteristic is the radiation pattern. Figure 12 shows the E- and H-plane patterns at 6 GHz and 8 GHz. The radiation is omnidirectional. Some discrepancies can be found due to the

TABLE 1. Comparison of the recently reported UWB-MIMO antennas.

Ref #	Size [mm^2] ($l \times w$)	Size ($\lambda_g \times \lambda_g$)	Frequency [GHz]	Isolation [dB]	ECC	Diversity Gain (dB)
[16]	30×50	1.09×1.82	2.5—14.5	< -20	<0.04	>7.5
[17]	50×80	1.65×2.65	3.1—10.6	< -17	< 0.056	NA
[18]	30×40	1.09×1.46	2.4,3.1—10.6	< -11.5	< 0.15	NA
[24]	40×50	1.46×1.82	2.5—11	< -15	< 0.02	NA
[25]	60×40	2.19×1.46	3.1—10.6	< -20	< 0.06	> 9.89
[26]	37×46	1.01×1.26	2—10.6	< -20	< 0.02	> 9.9
This work	25×32	0.91×1.17	3.1—10.6	<-20	< 0.005	> 9.99

* Here, λ_g denotes the antenna size in term of the guided wavelength (defined by 50 Ω impedance feed line operating at 6 GHz) corresponding to the substrate properties.

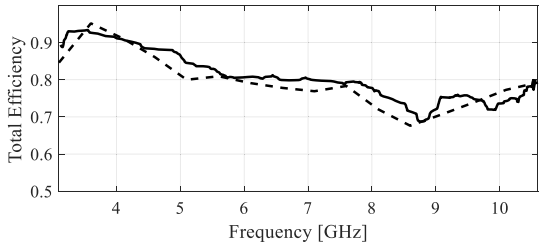

FIGURE 11. Simulated and measured total efficiency of the optimized UWB-MIMO antennas with the two-section slit below the feed line: Simulated (- - -), and Measured ones (—).

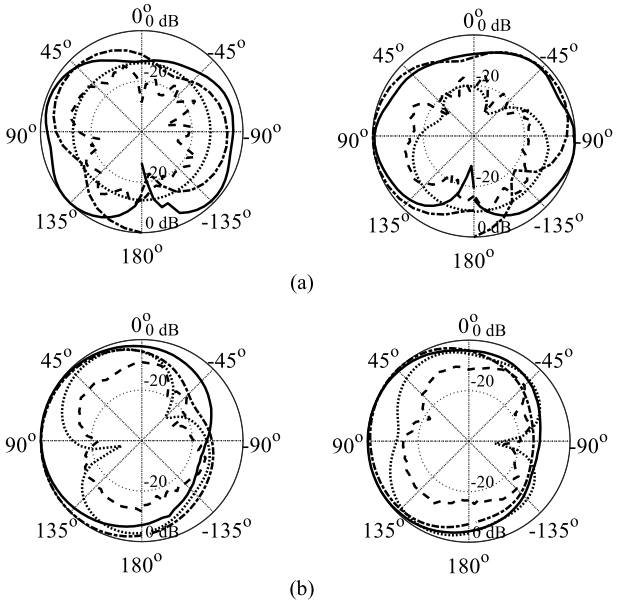

FIGURE 12. Simulated and measured radiation pattern of the optimized UWB-MIMO antenna with the two-section slit below the feed line: Simulated co-pol (- - -), measured co-pol (—), simulated cross-pol (...) and measured cross-pol (– – –). The plots from left- to right- hand side are for the frequencies 6 GHz and 8 GHz: (a) E- and (b) H-plane.

substrate characteristics, and (especially for the E plane) due to utilization of the 90-degree bend to mount the antenna.

IV. CONCLUSION

In this paper, a technique for isolation improvement of compact wideband MIMO antennas has been proposed, and demonstrated using an exemplary UWB MIMO structure. High isolation was achieved by using an n-section slit below the feed line. Systematic ground plane modifications have been investigated leading to a conclusion that $n = 2$ gives an optimum trade-off between the structure complexity and performance. Also, rigorous design closure of the antenna has been carried out using numerical optimization to ensure its best possible performance. The measured results ($|S_{21}| \leq -20$ dB, ECC < 0.005, DG > 9.99dB) confirm suitability of the antenna for modern communication systems. The considered structure also exhibits satisfactory field properties, in particular, high efficiency and omnidirectional radiation characteristics. The presented work can be used as a benchmark for future investigations of the impact of specific topology alterations on MIMO antenna performance.

ACKNOWLEDGMENT

The authors thank Dassault Systemes, France, for making CST Microwave Studio available.

REFERENCES

[1] C. M. Wu, Y. L. Chen, and W. C. Liu, "A compact ultrawideband slotted patch antenna for wireless USB dongle application," *IEEE Antennas Wireless Propag. Lett.*, vol. 11, pp. 596–599, 2012.
[2] H. Bahramiabarghouei, E. Porter, A. Santorelli, B. Gosselin, M. Popović, and L. A. Rusch, "Flexible 16 antenna array for microwave breast cancer detection," *IEEE Trans. Biomed. Eng.*, vol. 62, no. 10, pp. 2516–2525, Oct. 2015.
[3] *Federal Communications Commission Revision of Part 15 of the Commission's Rules Regarding Ultrawideband Transmission System From 3.1 to 10.6 GHz*, document ET-Docket 98-153, Federal Communications Commission, Washington, DC, USA, 2002.
[4] Q. H. Abbasi, M. U. Rehman, X. Yang, A. Alomainy, K. Qaraqe, and E. Serpedin, "Ultrawideband band-notched flexible antenna for wearable applications," *IEEE Antennas Wireless Propag. Lett.*, vol. 12, pp. 1606–1609, 2013.
[5] A. Bekasiewicz and S. Koziel, "Compact UWB monopole antenna for Internet of Things applications," *Electron. Lett.*, vol. 52, no. 7, pp. 492–494, 2016.
[6] G. Srivastava, A. Mohan, and A. Chakrabarty, "Compact reconfigurable UWB slot antenna for cognitive radio applications," *IEEE Antennas Wireless Propag. Lett.*, vol. 16, pp. 1139–1142, 2017.
[7] S. Koziel and A. Bekasiewicz, "Electromagnetic-simulation-driven design of compact ultra-wideband multiple-input–multiple-output antenna," *IET Microw., Antennas Propag.*, vol. 10, no. 15, pp. 1721–1724, 2016.
[8] S. Tripathi, A. Mohan, and S. Yadav, "A compact Koch fractal UWB MIMO antenna with WLAN band-rejection," *IEEE Antennas Wireless Propag. Lett.*, vol. 14, pp. 1565–1568, 2015.
[9] P.-S. Kildal and K. Rosengren, "Correlation and capacity of MIMO systems and mutual coupling, radiation efficiency, and diversity gain of their antennas: Simulations and measurements in a reverberation chamber," *IEEE Commun. Mag.*, vol. 42, no. 12, pp. 104–112, Dec. 2004.
[10] S. Koziel, A. Bekasiewicz, and Q. S. Cheng, "Conceptual design and automated optimisation of a novel compact UWB MIMO slot antenna," *IET Microw., Antennas Propag.*, vol. 11, no. 8, pp. 1162–1168, 2017.
[11] L. Liu, S. W. Cheung, and T. I. Yuk, "Compact MIMO Antenna for portable devices in UWB applications," *IEEE Trans. Antennas Propag.*, vol. 61, no. 8, pp. 4257–4264, Aug. 2013.
[12] Z. Li, Z. Du, M. Takahashi, K. Saito, and K. Ito, "Reducing mutual coupling of MIMO antennas with parasitic elements for mobile terminals," *IEEE Trans. Antennas Propag.*, vol. 60, no. 2, pp. 473–481, Feb. 2012.
[13] Q. Li, A. P. Feresidis, M. Mavridou, and P. S. Hall, "Miniaturized double-layer EBG structures for broadband mutual coupling reduction between UWB monopoles," *IEEE Trans. Antennas Propag.*, vol. 63, no. 3, pp. 1168–1171, Mar. 2015.
[14] S. Zhang and G. F. Pedersen, "Mutual coupling reduction for UWB MIMO antennas with a wideband neutralization line," *IEEE Antennas Wireless Propag. Lett.*, vol. 15, pp. 166–169, 2016.
[15] R. Anitha, V. P. Sarin, P. Mohanan, and K. Vasudevan, "Enhanced isolation with defected ground structure in MIMO antenna," *Electron. Lett.*, vol. 50, no. 24, pp. 1784–1786, 2014.
[16] A. Iqbal, O. A. Saraereh, A. W. Ahmad, and S. Bashir, "Mutual coupling reduction using F-shaped stubs in UWB-MIMO antenna," *IEEE Access.*, vol. 6, pp. 2755–2759, 2018.
[17] S. S. Jehangir and M. S. Sharawi, "A miniaturized UWB biplanar Yagi-like MIMO antenna system," *IEEE Antennas Wireless Propag. Lett.*, vol. 16, pp. 2320–2323, 2017.
[18] J.-Y. Deng, L.-X. Guo, and X.-L. Liu, "An ultrawideband MIMO Antenna with a high isolation," *IEEE Antenna Wireless Propag. Lett.*, vol. 15, pp. 182–185, 2016.
[19] S. Koziel and M. A. Ul Haq, "Ground plane modifications for design of miniaturised UWB antennas," *IET Microw., Antennas Propag.*, vol. 12, no. 8, pp. 1360–1366, 2018.
[20] *CST Microwave Studio, Version 2015*. CST AG, Darmstadt, Germany, 2015.

[21] S. Koziel, "Computationally efficient multi-fidelity multi-grid design optimization of microwave structures," *Appl. Comput. Electromagn. Soc. J.*, vol. 25, no. 7, pp. 578–586, 2010.
[22] A. R. Conn, N. I. M. Gould, and P. L. Toint, *Trust Region Methods* (MPS-SIAM Series on Optimization). Philadelphia, PA, USA: MPS, 2000.
[23] S. Blanch, J. Romeu, and I. Corbella, "Exact representation of antenna system diversity performance from input parameter description," *Electron. Lett.*, vol. 39, no. 9, pp. 705–707, May 2003.
[24] G.-S. Lin, C.-H. Sung, J.-L. Chen, L.-S. Chen, and M.-P. Houng, "Isolation improvement in UWB MIMO antenna system using carbon black film," *IEEE Antennas Wireless Propag. Lett.*, vol. 16, pp. 222–225, 2017.
[25] C.-X. Mao, Q.-X. Chu, Y.-T. Wu, and Y.-H. Qian, "Design and investigation of closely-packed diversity UWB slot-antenna with high isolation," *Prog. Electromagn. Res. C*, vol. 41, pp. 13–25, 2013.
[26] S. U. Kharche, G. S. Reddy, B. Mukherjee, R. K. Gupta, and J. Mukherjee, "MIMO antenna for Bluetooth, Wi-Fi, Wi-MAX and UWB applications," *Prog. Electromagn. Res. C*, vol. 52, pp. 53–62, 2014.

MUHAMMAD AZIZ UL HAQ received the B.S. and M.S. degrees in electronic engineering from Mohammad Ali Jinnah University, Karachi (Islamabad campus), Pakistan, in 2011 and 2014, respectively. He is currently pursuing the Ph.D. degree with the School of Science and Engineering, Reykjavík University, Iceland. He has been involved in several projects in the field of contemporary antenna design for microwave imaging, eHealth, and future wireless communication systems, such as 5G and Internet of Things, from 2014 to 2016. His research interests include compact antenna design and optimization methods for selected classes of antenna structures.

SLAWOMIR KOZIEL received the M.Sc. and Ph.D. degrees in electronic engineering from the Gdansk University of Technology, Poland, in 1995 and 2000, respectively, the M.Sc. degree in theoretical physics and the M.Sc. and Ph.D. degrees in mathematics from the University of Gdansk, Poland, in 2000, 2002, and 2003, respectively. He is currently a Professor with the School of Science and Engineering, Reykjavík University, Iceland. His research interests include CAD and modeling of microwave and antenna structures, simulation-driven design, surrogate-based optimization, space mapping, circuit theory, analog signal processing, evolutionary computation, and numerical analysis.